

1 **Adrift.org.au – a free, quick and easy tool to quantitatively study**
2 **planktonic surface drift in the global ocean**

3 Erik van Sebille¹

4 ¹ ARC Centre of Excellence for Climate System Science, School of Biological, Earth
5 and Environmental Sciences, University of New South Wales, Sydney, Australia

6 Corresponding Author: Erik van Sebille, Faculty of Science, University of New
7 South Wales, Sydney, NSW 2052, Australia (E.vanSebille@unsw.edu.au; +61 2
8 9385 7196)

9 **Abstract:**

10 Almost all organisms in the ocean are impacted by ocean currents. Hence, there
11 is growing interest by marine ecologists in using objective methods to assess
12 current drift and its implications for marine connectivity. Here, an online tool –
13 hosted at adrift.org.au – is introduced that allows for a simple, quantitative
14 assessment of drift patterns and transit time scales on the global scale. The tool
15 is based on a statistical transition matrix representation of the observed
16 trajectories of more than 15 thousand surface drifters. Users can select any point
17 in the ocean and obtain the evolution of the probability density distribution for a
18 tracer released at that point, both forward and backward in time, for a maximum
19 interval of 10 years. It is envisioned that this tool will be used in research and
20 teaching, especially where estimates of drift patterns and transit times are
21 required quickly.

22 **Keywords:** Ocean circulation, dispersion, drifting buoys

23 **1. Introduction**

24 Many organisms in the ocean are planktonic for either their entire lifespan or
25 during some stage of their life cycle (e.g. Suthers and Rissik, 2009). This means
26 that these species – including bacteria (e.g. Wilkins et al., 2013), foraminifera
27 (e.g. Weyl, 1978) and jellyfish (e.g. Dawson et al., 2005) as well as eggs and
28 larvae of fish (Aiken et al., 2011; e.g. Cowen et al., 2006; White et al., 2010),
29 crustaceans (e.g. Griffin et al., 2001) and algae (e.g. Coleman et al., 2013) – can
30 drift and disperse over long distances during their life. In addition, stronger
31 swimmers such as nekton, including large fish, turtles, marine mammals and
32 penguins may have their movements impacted by currents that can alter their
33 speed of travel or carry individuals off-course (see Chapman et al., 2011 for a
34 review).

35 Understanding this pelagic drift is important for studying (genetic) connectivity,
36 species invasion, biogeography or for explaining animal behaviour (such as in
37 some species of turtle; Scott et al., 2014). Given this broad impact of ocean
38 currents, it is not surprising that biologists have had a long interest in assessing
39 the implications of current drift for their particular species or ecosystems of
40 interest. Many decades ago, marine biologists used simple schematics of ocean
41 currents to assess ocean drift (Carr, 1967), thereby ignoring the variability in
42 currents and details such as eddies. As ocean current models and trajectories of
43 drifting buoys started to become available, there were efforts by biologists to
44 use these tools (e.g. Hays and Marsh, 1997).

45 Studies in the early 1990s were constrained by the limitations of the models and
46 the availability and extent of buoy trajectories. The last 20 years have seen

47 advances in both areas. Ocean models are now widely used by biologists (Cowen
48 et al., 2006; e.g. Hays et al., 2013; Kough et al., 2013; Naro-Maciel et al., 2014;
49 Paris et al., 2005; Simpson et al., 2013; Staaterman et al., 2012). However, these
50 ocean models still do not reproduce all the details and variability in actual ocean
51 currents and require a skills set to implement that is often outside the
52 experience of marine ecologists (Fossette et al., 2012). At the same time, the
53 freely available data-set of global Lagrangian drifter trajectories has grown
54 hugely (<http://www.aoml.noaa.gov/phod/dac/index.php>) and this is now a relatively
55 straightforward resource for biologists to use in its simplest form of plotting
56 individual trajectories (Monzon-Argueello et al., 2010).

57 Here I describe a freely available, quick and simple online tool for studying the
58 pathways and time scales of ocean surface drift based on empirical data. The tool
59 uses Lagrangian drifter data but goes well beyond plotting individual
60 trajectories. Rather, the tool splices together all the possible drift scenarios in
61 the Lagrangian drifter dataset so that the full extent of drift scenarios is
62 generated and quantified. This easy-to-implement approach promises to have
63 very wide utility (van Sebille et al., 2011; 2012a), although there are some
64 caveats (including the lack of control over exact depth habitat of the organisms
65 and the absence of mortality or settling/beaching, see also the Discussions and
66 Conclusion section) that might limit the merit of the tool for certain research
67 questions.

68 The website adrift.org.au is fronted by an easy-to-use interface (Figure 1) where
69 researchers can study the movement (in a probabilistic sense) of passive
70 particles from any point in the ocean, both forward and backward in time. While

71 adrift.org.au is framed in terms of marine plastics, the results are equally
72 representative for many planktonic species in the upper few meters of the ocean.
73 Output from the website can be downloaded in comma separated values (csv)
74 format for easy import into data analysis programs like Microsoft Excel, R,
75 python or Mathworks Matlab.

76 **2. The methodology behind adrift.org.au**

77 *2.1 The surface drifter data*

78 The numerical engine behind adrift.org.au is built on an updated version of the
79 methodology described in (van Sebille et al., 2012a), which is similar to that
80 presented in (Maximenko et al., 2012). In these studies, the trajectories of
81 surface drifters (Niiler, 2001), as aggregated in the NOAA Global Drifting Buoy
82 Program (Lumpkin, 2003; Lumpkin et al., 2012), were used to study the
83 formation and evolution of the marine garbage patches. In total, more than 24
84 million locations from 17,494 individual surface drifter trajectories and
85 spanning a time period between 1979 and 2013 are used on adrift.org.au. The
86 drifter geolocations are available every 6 hours, and more than 85% of the ocean
87 surface has had more than 100 location fixes per 1° x 1° degree grid cell during
88 that 34 year period (van Sebille et al., 2011). See Figure 2 for an example of the
89 density of drifter trajectories.

90 The buoys are deployed with a drogue centered at 15m depth, which is there to
91 make the buoys less prone to windage effects and hence more closely follow the
92 (upper-ocean) Ekman transport. However, many buoys lose their drogue at
93 some point, affecting their paths (Grotsky et al., 2011; Poulain et al., 2009).

94 Within the data set used here, 48% of all data used is of buoys with a drogue and
95 52% is of buoys without a drogue, making the data representative for anything
96 that drifts in the upper 15m of the ocean. Maximenko et al. (2012) showed that
97 although the details of the pathways of drogued and undrogued buoys are
98 different, the evolution of the two types of buoys is similar on longer timescales
99 and larger spatial scales. Furthermore, it can be argued that neutrally buoyant
100 particles that constantly change depth within the mixed layer will have
101 pathways that are a mix of both the drogued and undrogued buoys.

102 *2.2 The global transition matrix*

103 As in Van Sebille et al. (2012a), the drifter trajectories are converted into a set of
104 six transition matrices (Dellnitz et al., 2009; Froyland et al., 2007) that
105 represent, for each surface grid cell on the ocean, the fractional distribution of
106 tracer two months later. More specifically (see also Figure 3), each individual
107 drifter trajectory is binned onto a $1^\circ \times 1^\circ$ degree array of grid cells. For each
108 trajectory and then within each trajectory for each day t , the number of times a
109 buoy crosses from grid cell i at time t to grid cell j at time $t + \Delta t$ is added to the
110 crossing matrix $C_b(i,j)$. Here, we use $\Delta t = 2$ months and a grid size of 1° , which
111 are the same values as used in Van Sebille et al. (2012a). The choice for a $1^\circ \times 1^\circ$
112 grid is an optimum between the size of the matrix (and hence computational
113 effort) and the ability to resolve fronts, as also shown in Van Sebille et al. (2011).
114 The choice for $\Delta t = 2$ months ensures both a sufficient number of off-diagonal
115 crossings (which requires a Δt larger than 1 month) and a good representation
116 of seasonality (which requires a Δt smaller than 3 months). The seasonal cycle in
117 the circulation is resolved by classifying the time of year each crossing occurred

118 and then adding that crossing to one of six crossing matrices for each two-month
119 period (Jan-Feb for \mathbf{C}_1 , Mar-Apr for \mathbf{C}_2 , ..., Nov-Dec for \mathbf{C}_6).

120 The crossing matrices \mathbf{C}_b are converted to transition matrices \mathbf{P}_b by row-
121 normalizing them (i.e. making the sum of each row i equal to 1.0). The entries in
122 the rows of \mathbf{P}_b can be interpreted as a 2-dimensional probability distribution of a
123 virtual tracer two month after it is released from a grid cell. Ocean grid cells that
124 buoys have never reached or have never exited from are removed from the
125 transition matrix. The total number of ocean grid cells that remains in this way is
126 $N = 33,654$, and they are ordered from south to north. The transition matrix for
127 the months January and February (\mathbf{P}_1 , Figure 2b) is rather diagonal and sparse,
128 indicating that for each grid cell (each row in \mathbf{P}_b), there are only a limited
129 amount of grid cells within the vicinity that are reachable in two months. This
130 transition matrix also shows that dispersion is larger in the Southern Ocean
131 around 60°S than anywhere else, largely because of the large speeds and eddy
132 activity there.

133 The general idea of the tool is that each transition matrix calculates the
134 probabilities that a particle that is in one grid cell at time t has moved to any of
135 the grid cells by time $t + 2$ months. This calculation is then repeated through
136 time, so that for a particle at $t + 2$ months that has moved to a new grid cell, the
137 subsequent probability of moving to all other cells is estimated and so forth.
138 Numerically, the evolution of the probabilities v from any point in the ocean can
139 be computed by solving the iterative vector-matrix multiplication $v_{t+2\text{months}} = v_t \times$
140 \mathbf{P}_b where the bimonthly counter b is cycled through.

141 The initial condition on adrift.org.au is that $v_{t=0} = 0$ everywhere except for the
142 entry i that represents the grid cell where the user clicked, which is $v_{t=0}(i) = 1$.
143 Releases in different two-month periods can be simulated by using a different
144 initial value of the counter b at $t = 0$. Because of the row-normalisation, the
145 virtual tracer is conserved throughout the iteration, meaning that the total
146 probability of the particles being somewhere in the ocean will always be 1. This
147 means that the tool doesn't account for mortality, beaching or other ways in
148 which a particle might leave the ocean.

149 *2.3 Hybrid transition matrices for regional experiments*

150 While the surface drifter data set is adequate for the study of tracer evolution in
151 the open ocean, where the number of samples is generally large, it is not
152 sufficient in some regional seas such as for instance the Indonesian Archipelago
153 or the Strait of Gibraltar. In the 30 years since the global drifter program started,
154 for example, there has never once been a surface buoy that has crossed the
155 Indonesian Archipelago (Lumpkin et al., 2012).

156 Because of this lack of observational data in some regional areas, hybrid
157 transition matrices \mathbf{P}_b are created for the regional experiments only. These
158 hybrid transition matrices are formed from a combination of both the
159 observational drifting buoy trajectories and a set of virtual particles released
160 within a numerical ocean circulation model. The model is the eddy resolving
161 OFES model data set (Masumoto et al., 2004), with a horizontal resolution of 0.1°
162 and 54 vertical levels. This model, although lacking the sub-mesoscale structures
163 that do affect the drifting buoys, has been shown to accurately reproduce the
164 circulation in many areas of the global ocean (Masumoto et al., 2004; Sasaki et

165 al., 2008), as well as in specific regions such as around Australia (van Sebille et
166 al., 2012b). For the analysis here, the 2-dimensional horizontal velocity at 15 m
167 depth (the nominal depth of the surface drifters) from the model has been used.
168 A total of 455,236 virtual particles were released within the velocity fields in the
169 year 1980, on a $1^\circ \times 1^\circ$ grid and every 30 days. The locations of the particles were
170 saved every 6 hours, and the particles were advected for a total of 365 days,
171 using the Connectivity Modeling System version 1.1 (Paris et al., 2013).

172 The trajectories of the virtual particles were also converted into a crossing
173 matrix $\mathbf{C}_{b\text{model}}$. Before normalizing the crossing matrices, however, they were
174 entry-wise added together as $\mathbf{C}_b(i,j)_{\text{hybrid}} = \mathbf{C}_b(i,j)_{\text{model}} + w * \mathbf{C}_b(i,j)_{\text{obs}}$, using a
175 weighing factor w of 10. This weighing factor ensures that, in the regional
176 transition matrices, the hybrid transition distribution is very similar to the
177 observed transition distribution for regions where sufficient surface drifters are
178 available, and that the model trajectories are only used in regions where
179 observed drifter coverage is inadequate.

180 **3. Using adrift.org.au**

181 Users of adrift.org.au are presented with a map of the global ocean. The mouse is
182 used to select a point somewhere in the ocean that represents the start point of
183 the particles. After a few seconds, an animated simulation is produced that
184 shows how tracer from that location spreads through the ocean (Figure 1). Each
185 frame in the animation represents an interval of 2 months, and the total
186 animation runs for 10 years, a time ceiling currently dictated by limits on the
187 computational resources.

188 The simulation represents the evolution of a large number of free drifting,
189 neutrally buoyant particles, with the color scale indicating the percentage of
190 particles in each 1° x 1° grid cell at each time interval. As dispersion causes the
191 density of particles to decrease rapidly in the ocean, the colour scale (bottom
192 right) has a maximum value of 1% of the total amount of particles. The value in
193 each grid cell can be viewed as a probability that a particle is found in that grid
194 cell, a certain amount of time after being released.

195 The particles can be tracked both forward in time (the default) and backwards in
196 time, by toggling the switch on the map. In the latter case, the animation shows
197 the probability distribution of where particles at the selected location have come
198 from. There is also an option on the map to zoom into specific regions. Currently,
199 only the Mediterranean and the seas around Australia are available, but new
200 regions will be added in the future.

201 After the animation has finished, users are able to download the simulation data
202 in a comma separated values (csv) format as (year, month, latitude, longitude,
203 probability). These files can be loaded into other software and used to further
204 investigate the quantitative spreading of the particles (see also Section 4). Users
205 who want to have more precise control of where the particles are released can
206 alter the start location manually in the browser's address bar, using the format
207 `adrift.org.au/map?lat=LAT&lng=LNG&startmon=MON`, where LAT and LNG are numerical
208 values of latitude and longitude, respectively, and MON is the three-letter
209 abbreviation of the month. Note that, since the method works with bimonthly
210 increments, JAN is the same as FEB, APR is the same as MAR, etc.

211 **4. An example: drift times across the North Atlantic**

212 As an example of how adrift.org.au can be used, the fastest-possible drift across
213 the North Atlantic from the US East Coast is examined. For this, the simulation at
214 adrift.org.au/map?lat=35&lng=-75¢er=251.4&startmon=Jan has been downloaded in
215 csv format. Some simple manipulation of the csv file allows for the creation of a
216 map that for example shows the shortest transit times from Cape Hatteras to any
217 point in the Atlantic Ocean (Figure 4). On this map, which is coloured on a
218 logarithmic scale to highlight differences in timing in the first few months after
219 release, regions that are white cannot be reached within 10 years.

220 The cyclonic circulation of the subtropical gyre is very clear in the map, with
221 transit time scales of less than 2 years in the Gulf Stream extension and North
222 Atlantic Current, increasing to 2 to 4 years on the southern flank of the
223 subtropical gyre around 20°S. Fastest times to cross the North Atlantic and reach
224 Europe are in the order of 1.5 years, which agrees well with direct analysis of the
225 drifter trajectories (Brambilla and Talley, 2006) and numerical ocean modelling
226 studies (Baltazar-Soares et al., 2014). As also found in these studies, as well as in
227 another recent numerical ocean modelling study (Burkholder and Lozier, 2014),
228 there is very little mixing between the subtropical gyre and the subpolar gyre,
229 with a very sharp front between the North Atlantic Current and the subpolar
230 gyre to the northwest. This suggests, as was also shown in van Sebille et al.
231 (2011), that the effect of spurious cross-frontal diffusion in the transition matrix
232 approach is limited.

233 Note that the map in Figure 4 is rather noisy in some regions such as the Gulf of
234 Mexico and northeast of Iceland. This is related to very low probabilities to reach
235 these grid points from Cape Hatteras. If a more smoothed version of this figure is

236 required, grid cells with very low probability of reaching could be blanked out.
237 The analysis using adrift.org.au shows that it is possible to reach the Barents Sea,
238 but that from Cape Hatteras it takes at least three to four years to reach that
239 area.

240 An analysis such as this one can be very useful as a way for marine biologist to
241 quickly get an idea of the dispersion range of a particular species, given the span
242 of its planktonic life. Note that in this example any particle density greater than 0
243 was taken as significant. It is relatively straightforward to change the analysis to
244 include a threshold probability; for example a one in a thousand chance of
245 reaching a certain area.

246 **5. Discussions and Conclusion**

247 Adrift.org.au is a free, easy to use tool that can help marine biologists and
248 ecologists quickly assess drift pathways in the global ocean. Although the
249 website started as a public outreach tool, the methodology behind the website is
250 scientifically robust. The narrative of the website is whimsical (featuring lots of
251 rubber ducks: a reference to the story of the container full of bath toys lost at sea
252 - Ebbesmeyer and Scigliano, 2009) and focuses on the problem of marine litter.
253 However, the tool can be used beyond the study of pathways of plastics. The drift
254 of many different substances, including planktonic marine organisms, can be
255 studied using the same statistical analysis of observational drifting buoy
256 trajectories.

257 The method is different from most other tracking tools available (e.g. Condie,
258 2005; Lett et al., 2008; Paris et al., 2013) in that - for the global version - it is

259 based entirely on empirical data. While this means that there are no errors
260 associated with numerical ocean models or the choices for parameters
261 associated with running virtual particles in these models (Putman and He, 2013;
262 Simons et al., 2013), the method does have some caveats that users should be
263 aware of. These include the fact that a mix both drogued and undrogued drifters
264 is used and that therefore the user doesn't have control of the exact depth
265 habitat of the organisms. It is hoped that, as the global drifter dataset increases
266 in size, coverage will within a few years be sufficient to construct transition
267 matrices of the drogued and undrogued drifters separately, so that users can
268 choose which depth scenario most suits their needs.

269 The method behind adrift.org.au is also different from most other tracking
270 methods in that pathways are inherently statistical, and that contrary to direct
271 integration methods users don't get individual trajectories to analyze. Finally,
272 the limits of the observed data set mean that the resolution of the global run is
273 only 1° x 1°, which is relatively coarse for organisms with short drift durations.
274 Nevertheless, it is hoped that adrift.org.au is a valuable addition to the landscape
275 of tracking tools and that the site will be used by scientists, both in their teaching
276 and their research, who are interested in how ocean currents shape ecosystems.

277

278 **Acknowledgements:** This project was supported by the Australian Research
279 Council via grants DE130101336 and CE110001028. Jack Murray and David
280 Fuchs are thanked for their help in developing [adrift](http://adrift.org.au). Prof Graeme Hays and Dr
281 Alex Sen Gupta are thanked for their discussions on the potential of adrift.org.au

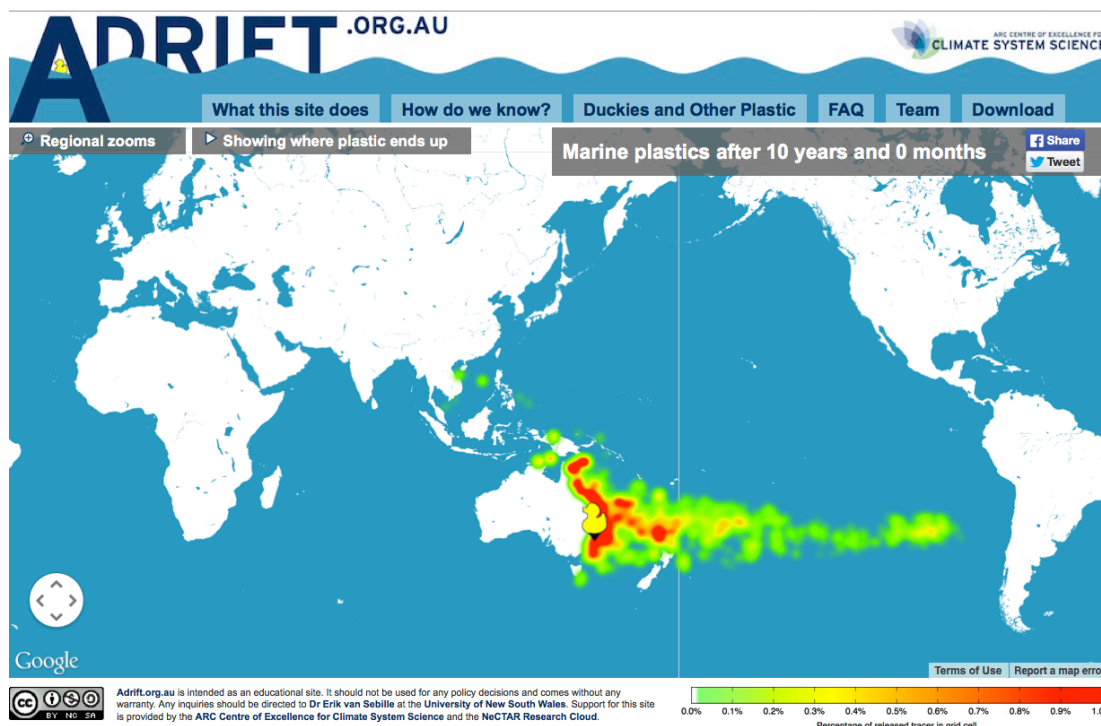
282 in scientific research. Comments from three anonymous reviewers have greatly
283 improved this manuscript.

284 **References**

- 285 Aiken, C.M., Navarrete, S.A., Pelegrí, J.L., 2011. Potential changes in larval
286 dispersal and alongshore connectivity on the central Chilean coast due to an
287 altered wind climate. *J Geophys Res* 116, G04026.
288 doi:10.1029/2011JG001731
- 289 Baltazar-Soares, M., Biastoch, A., Harrod, C., Hanel, R., Marohn, L., Prigge, E.,
290 Evans, D., Bodles, K., Behrens, E., Böning, C.W., 2014. Recruitment collapse
291 and population structure of the European eel shaped by local ocean current
292 dynamics. *Current Biology* 24, 104–108. doi:10.1016/j.cub.2013.11.031
- 293 Brambilla, E., Talley, L.D., 2006. Surface drifter exchange between the North
294 Atlantic subtropical and subpolar gyres. *J Geophys Res* 111, C07026.
295 doi:10.1029/2005JC003146
- 296 Burkholder, K.C., Lozier, M.S., 2014. Tracing the pathways of the upper limb of
297 the North Atlantic Meridional Overturning Circulation. *Geophysical Research*
298 *Letters*. doi:10.1002/(ISSN)1944-8007
- 299 Carr, A.F., 1967. *So Excellent a Fish: a Natural History of Sea Turtles*. Natural
300 History Press.
- 301 Chapman, J.W., Klaassen, R.H.G., Drake, V.A., Fossette, S., Hays, G.C., Metcalfe, J.D.,
302 Reynolds, A.M., Reynolds, D.R., Alerstam, T., 2011. Animal Orientation
303 Strategies for Movement in Flows. *Current Biology* 21, R861–R870.
304 doi:10.1016/j.cub.2011.08.014
- 305 Coleman, M.A., Feng, M., Roughan, M., Cetina-Heredia, P., Connell, S.D., 2013.
306 Temperate shelf water dispersal by Australian boundary currents:
307 Implications for population connectivity. *Limnology & Oceanography: Fluids*
308 *& Environments* 3, 295–309. doi:10.1215/21573689-2409306
- 309 Condie, S., 2005. Web site on marine connectivity around Australia. *Eos Trans.*
310 *AGU* 86, 246. doi:10.1029/2005E0260006
- 311 Cowen, R.K., Paris, C.B., Srinivasan, A., 2006. Scaling of connectivity in marine
312 populations. *Science* 311, 522–527. doi:10.1126/science.1122039
- 313 Dawson, M.N., Gupta, A.S., England, M.H., 2005. Coupled biophysical global ocean
314 model and molecular genetic analyses identify multiple introductions of
315 cryptogenic species. *Proc. Natl. Acad. Sci. U.S.A.* 102, 11968–11973.
- 316 Dellnitz, M., Froyland, G., Horenkamp, C., Padberg-Gehle, K., Gupta, Sen, A., 2009.
317 Seasonal variability of the subpolar gyres in the Southern Ocean: a numerical
318 investigation based on transfer operators. *Nonlinear Proc Geoph* 16, 655–
319 663.
- 320 Ebbesmeyer, C.C., Scigliano, E., 2009. *Flotsametrics and the Floating World: How*
321 *One Man's Obsession with Runaway Sneakers and Rubber Ducks*
322 *Revolutionized Ocean Science*. Harper Collins.
- 323 Fossette, S., Putman, N.F., Lohmann, K.J., Marsh, R., Hays, G.C., 2012. A biologist's
324 guide to assessing ocean currents: a review. *Marine Ecology-Progress Series*
325 457, 285–301. doi:10.3354/meps09581
- 326 Froyland, G., Padberg, K., England, M.H., Treguier, A.-M., 2007. Detection of
327 coherent oceanic structures via transfer operators. *Phys Rev Lett* 98,

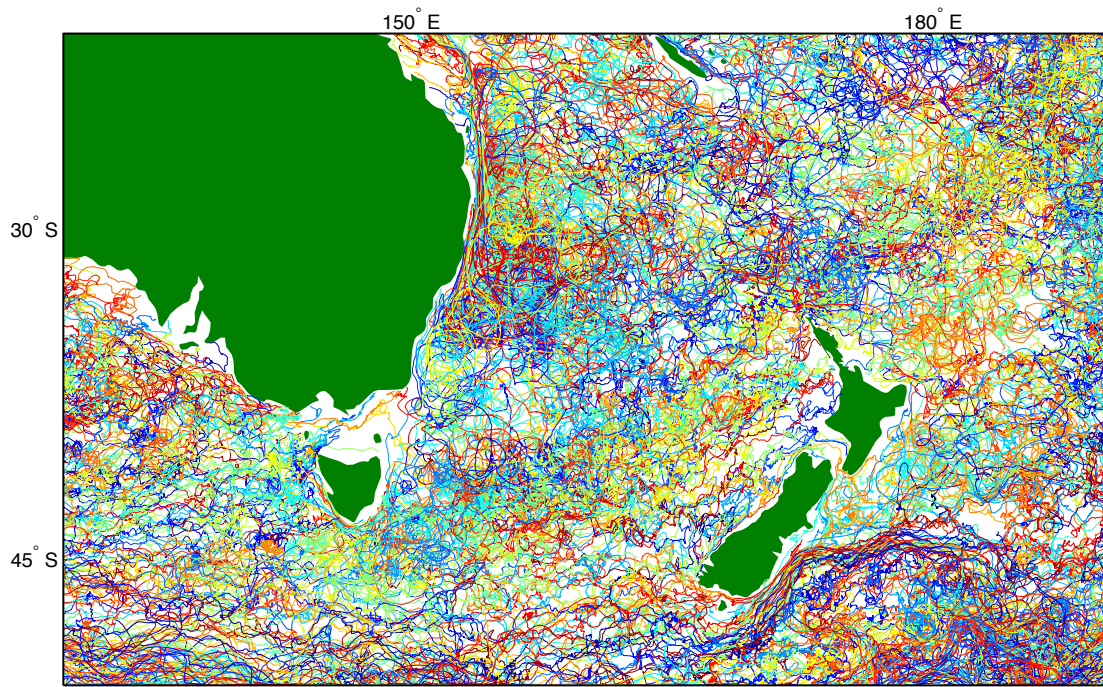
328 224503. doi:10.1103/PhysRevLett.98.224503
 329 Griffin, D.A., Wilkin, J.L., Chubb, C.F., Pearce, A.F., Caputi, N., 2001. Ocean currents
 330 and the larval phase of Australian western rock lobster, *Panulirus cygnus*.
 331 *Marine and Freshwater Research* 52, 1187–1199.
 332 Grodsky, S.A., Lumpkin, R., Carton, J.A., 2011. Spurious trends in global surface
 333 drifter currents. *Geophys Res Lett* 38, L10606. doi:10.1029/2011GL047393
 334 Hays, G.C., Christensen, A., Fossette, S., Schofield, G., Talbot, J., Mariani, P., 2013.
 335 Route optimisation and solving Zermelo's navigation problem during long
 336 distance migration in cross flows. *Ecol Lett* 17, 137–143.
 337 doi:10.1111/ele.12219
 338 Hays, G.C., Marsh, R., 1997. Estimating the age of juvenile loggerhead sea turtles
 339 in the North Atlantic. *Canadian Journal of Zoology-Revue Canadienne De*
 340 *Zoologie* 75, 40–46.
 341 Kough, A.S., Paris, C.B., Butler, M.J., IV, 2013. Larval Connectivity and the
 342 International Management of Fisheries. *PLOS One* 8, e64970.
 343 doi:10.1371/journal.pone.0064970.g001
 344 Lett, C., Verley, P., Mullon, C., Parada, C., Brochier, T., Penven, P., Blanke, B., 2008.
 345 A Lagrangian tool for modelling ichthyoplankton dynamics. *Environ Modell*
 346 *Software* 23, 1210–1214. doi:10.1016/j.envsoft.2008.02.005
 347 Lumpkin, R., 2003. Decomposition of surface drifter observations in the Atlantic
 348 Ocean. *Geophys Res Lett* 30, 1753. doi:10.1029/2003GL017519
 349 Lumpkin, R., Maximenko, N.A., Pazos, M., 2012. Evaluating where and why
 350 drifters die. *J Atmos Ocean Tech* 29, 300–308. doi:10.1175/JTECH-D-11-
 351 00100.1
 352 Masumoto, Y., Sasaki, H., Kagimoto, T., Komori, N., Ishida, A., Sasai, Y., Miyama, T.,
 353 Motoi, T., Mitsudera, H., Takahashi, K., Sakuma, H., Yamagata, T., 2004. A
 354 Fifty-Year Eddy-Resolving Simulation of the World Ocean - Preliminary
 355 Outcomes of OFES (OGCM for the Earth Simulator). *J Earth Simul* 1.
 356 Maximenko, N.A., Hafner, J., Niiler, P.P., 2012. Pathways of marine debris derived
 357 from trajectories of Lagrangian drifters. *Mar Pollut Bull* 65, 51–62.
 358 doi:10.1016/j.marpolbul.2011.04.016
 359 Monzon-Argueello, C., Lopez-Jurado, L.F., Rico, C., Marco, A., Lopez, P., Hays, G.C.,
 360 Lee, P.L.M., 2010. Evidence from genetic and Lagrangian drifter data for
 361 transatlantic transport of small juvenile green turtles. *Journal of*
 362 *Biogeography* 37, 1752–1766. doi:10.1111/j.1365-2699.2010.02326.x
 363 Naro-Maciel, E., Gaughran, S.J., Putman, N.F., Amato, G., Arengo, F., Dutton, P.H.,
 364 McFadden, K.W., Vintinner, E.C., Sterling, E.J., 2014. Predicting connectivity of
 365 green turtles at Palmyra Atoll, central Pacific: a focus on mtDNA and
 366 dispersal modelling. *Journal of The Royal Society Interface* 11.
 367 doi:10.1098/rsif.2013.0888
 368 Niiler, P.P., 2001. The world ocean surface circulation, in: Siedler, G., Church, J.A.,
 369 Gould, J. (Eds.), *Ocean Circulation and Climate: Observing and Modelling the*
 370 *Global Ocean*. Elsevier Oceanographic Series, pp. 193–204.
 371 Paris, C.B., Cowen, R.K., Claro, R., Lindeman, K.C., 2005. Larval transport
 372 pathways from Cuban snapper (*Lutjanidae*) spawning aggregations based on
 373 biophysical modeling. *Marine Ecology-Progress Series* 296, 93–106.
 374 Paris, C.B., Helgers, J., van Sebille, E., Srinivasan, A., 2013. Connectivity Modeling
 375 System: A probabilistic modeling tool for the multi-scale tracking of biotic
 376 and abiotic variability in the ocean. *Environ Modell Software* 42, 47–54.

377 doi:10.1016/j.envsoft.2012.12.006
378 Poulain, P.-M., Gerin, R., Mauri, E., Pennel, R., 2009. Wind Effects on Drogued and
379 Undrogued Drifters in the Eastern Mediterranean. *J Atmos Ocean Tech* 26,
380 1144–1156. doi:10.1175/2008JTECHO618.1
381 Putman, N.F., He, R., 2013. Tracking the long-distance dispersal of marine
382 organisms: sensitivity to ocean model resolution. *Journal of The Royal*
383 *Society Interface* 10, 20120979–20120979. doi:10.1098/rspb.2010.1088
384 Sasaki, H., Nonaka, M., Masumoto, Y., Sasai, Y., Uehara, H., Sakuma, H., 2008. High
385 Resolution Numerical Modelling of the Atmosphere and Ocean, in: Hamilton,
386 K., Ohfuchi, W. (Eds.). Springer New York, pp. 157–185.
387 Scott, R., Marsh, R., Hays, G., 2014. Ontogeny of long distance migration. *Ecology*.
388 Simons, R.D., Siegel, D.A., Brown, K.S., 2013. *Journal of Marine Systems. J Marine*
389 *Syst* 119-120, 19–29. doi:10.1016/j.jmarsys.2013.03.004
390 Simpson, S.D., Piercy, J.J.B., King, J., Codling, E.A., 2013. Modelling larval dispersal
391 and behaviour of coral reef fishes. *Ecological Complexity* 1–9.
392 doi:10.1016/j.ecocom.2013.08.001
393 Staaterman, E., Paris, C.B., Helgers, J., 2012. Orientation behavior in fish larvae A
394 missing piece to Hjort's critical period hypothesis. *J Theoret Biol* 304, 188–
395 196. doi:10.1016/j.jtbi.2012.03.016
396 Suthers, I., Rissik, D., 2009. *Plankton: A guide to their ecology and monitoring for*
397 *water quality*.
398 van Sebille, E., Beal, L.M., Johns, W.E., 2011. Advective time scales of Agulhas
399 leakage to the North Atlantic in surface drifter observations and the 3D OFES
400 model. *J Phys Oceanogr* 41, 1026–1034. doi:10.1175/2010JPO4602.1
401 van Sebille, E., England, M.H., Froyland, G., 2012a. Origin, dynamics and evolution
402 of ocean garbage patches from observed surface drifters. *Environ. Res. Lett.*
403 7, 044040. doi:10.1088/1748-9326/7/4/044040
404 van Sebille, E., England, M.H., Zika, J.D., Sloyan, B.M., 2012b. Tasman leakage in a
405 fine-resolution ocean model. *Geophys Res Lett* 39, L06601.
406 doi:10.1029/2012GL051004
407 Weyl, P.K., 1978. Micropaleontology and ocean surface climate. *Science* 202,
408 475–481.
409 White, C., Selkoe, K.A., Watson, J., Siegel, D.A., Zacherl, D.C., Toonen, R.J., 2010.
410 Ocean currents help explain population genetic structure. *Proceedings of the*
411 *Royal Society B: Biological Sciences* 277, 1685–1694.
412 Wilkins, D., van Sebille, E., Rintoul, S.R., Lauro, F.M., Cavicchioli, R., 2013.
413 Advection shapes Southern Ocean microbial assemblages independent of
414 distance and environment effects. *Nature Communications* 4, 1–7.
415 doi:10.1038/ncomms3457
416
417



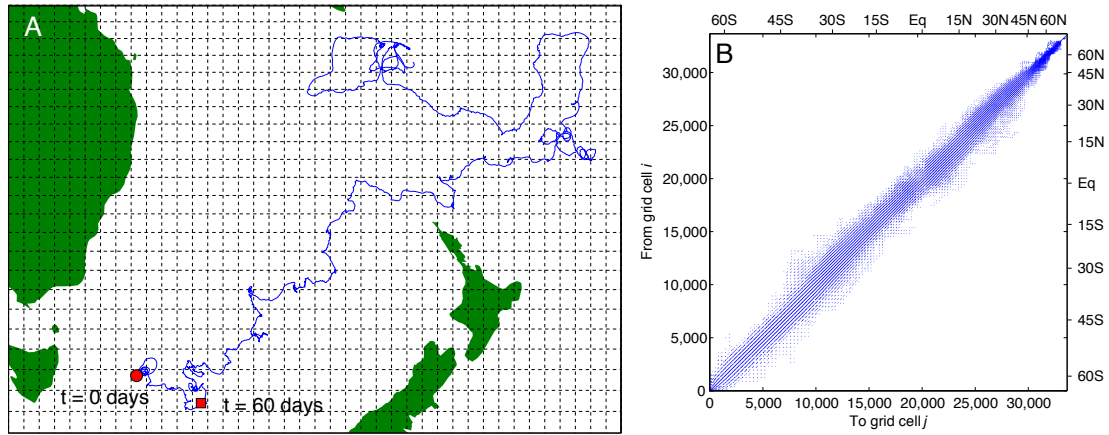
419

420 **Figure 1:** Screenshot of adrift.org.au, showing the distribution of tracer released
421 from a grid cell close to Sydney (where the black tip of the yellow duck points)
422 after 10 years. Colors are in percentages of the initial release, and capped at 1%
423 to visually highlight regions with relatively low concentrations. The download
424 button in the top right corner allows for the retrieval of a csv file that contains
425 the data from the simulation.



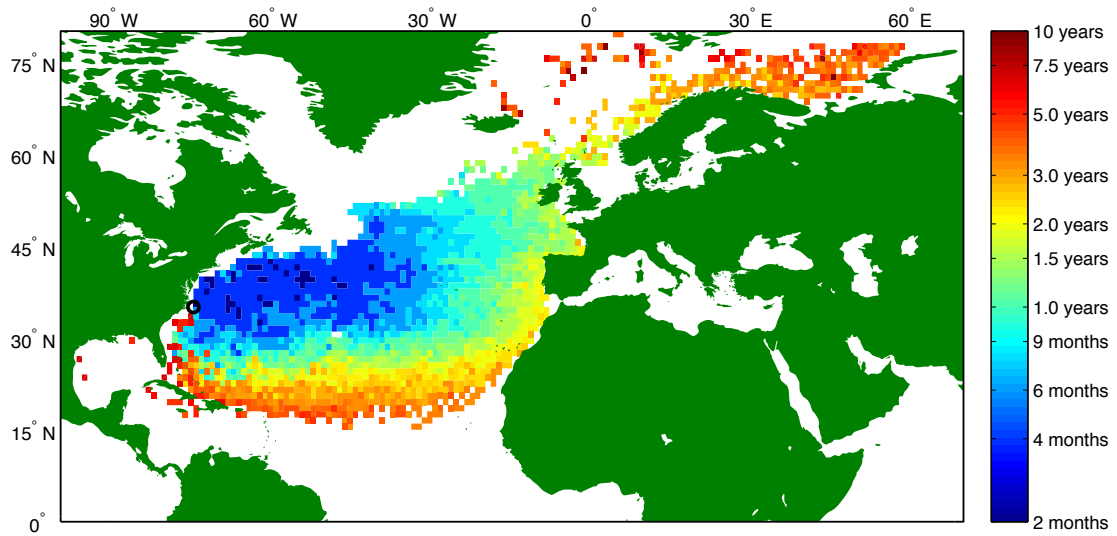
426

427 **Figure 2:** A map of all surface drifter trajectories ever to have passed through
428 the area between Eastern Australia and New Zealand. Each drifter has a unique,
429 randomly assigned, color. The drifters are geolocated every six hours. Although
430 there are some regions with fairly low coverage (such as Bass Strait between
431 southeast Australia and Tasmania, overall coverage is higher than 100 fixes per
432 $1^\circ \times 1^\circ$ grid cell. This is typical for most of the global ocean.



433

434 **Figure 3:** Depiction of the methodology to construct the transition matrix \mathbf{P}_b ,
 435 which is used to propagate the distribution of tracer forward in time. The $\mathbf{P}_b(i,j)$
 436 matrix is a row-normalized version of the crossing matrix $\mathbf{C}_b(i,j)$ which holds, for
 437 each pair of cells i and j , the number of times a surface drifter has moved from i
 438 to j in the two-month period b . a) Example how, for one drifter trajectory, two
 439 points are taken 60 days apart. This is done for each day along the trajectory. b)
 440 Depiction of the non-zero entries (in blue) of \mathbf{P}_1 , the global transition matrix for
 441 the months January and February. This matrix shows for a particular row (grid
 442 cell i), which columns (grid cells j) can be reached within 2 months. The ordering
 443 of the 33,654 grid cells is from south to north, and the ticks on the top and right
 444 of the panel show where some latitudes are located. Because there are more
 445 ocean grid cells in the Southern Hemisphere, this scale is non-linear.



446

447 **Figure 4:** Map of the minimum time it takes a particle released from Cape
 448 Hatteras (black circle) and passively drifting on the ocean surface to reach other
 449 areas in the North Atlantic. White areas cannot be reached in ten years,
 450 according to this analysis based on the observed surface buoy trajectories. Note
 451 that the color scale is logarithmic.